

# Recent LS-DYNA Developments in the Structural Conjugate Heat Transfer Solver

Thomas Klöppel

DYNAmore GmbH

## 1 Abstract

Increasing demands for the simulation of complex, multi-physics problems in crashworthiness and manufacturing process analyses have necessitated new developments in the structural conjugate heat transfer solver in LS-DYNA®. Some of the most recent extensions and new implementations are presented and discussed in this contribution.

The first block addresses the relatively new field of battery abuse simulations. Focus is put on a novel thermal composite thick shell element that is defined using `*PART_COMPOSITE_TSHELL`. On the one hand, the implementation allows for a relatively easy input definition. On the other hand, the formulation adds new temperature degrees of freedom for each layer of the composite structure and, thus, accurately resolves the internal lay-up of the structure, i.e. the battery cell. The reconstructed lay-up is also accounted for in the thermal contact routines. Consequently, the heat transfer through a stack of solid elements can be reproduced exactly by a single composite thick shell element with the corresponding lay-up definition.

The second block presents the work on different thermal boundary conditions. A recent enhancement enables the “standard” boundary conditions (convection, radiation, and flux) to be transferred to newly exposed surfaces after element erosion. In general, this is sufficient for modeling laser cutting with a flux boundary condition, but the input of such a model can become very complex. Therefore, a new thermal boundary condition `*BOUNDARY_FLUX_TRAJECTORY` is introduced in the second part of this block, which is tailored for moving heat sources acting on the surface of a structure. In contrast to the standard flux boundary condition, the new implementation also accounts for the tilting of the heat source. The boundary condition is applicable in coupled thermal-structural and thermal-only simulations.

The second block is completed by the presentation of a new temperature boundary condition `*BOUNDARY_TEMPERATURE_RSW` that is devised as a simplified modeling strategy for resistive spot welds (RSW). With the keyword, the temperature distribution in a weld nugget is defined directly.

## 2 Thermal Composite Thick Shell

### 2.1 Motivation

The development of thermal composite thick shell (tshell) elements has been necessary to meet new requirements by the automotive industry that are due to the increasing importance of electric vehicles. One key feature for an accurate numerical analysis of the crashworthiness of those cars is an accurate prediction of the multi-physics response of lithium-ion battery packs to abusive conditions. For that purpose at least the structural, the electro-magnetical and thermal behavior has to be taken into consideration.

The multi-physics nature of the problem leads to somewhat contradicting demands on the model set-up. On the one hand, electromagnetic (EM) and thermal solvers require a very fine resolution of the different layers of the battery cell. On the other hand, such a finely resolved model with potentially very different mechanical properties across the lay-up is unnecessarily challenging for the structural solver and drastically reduces the critical maximum time step of explicit time integration schemes. Moreover, the construction of such complex models is rather time-consuming for the user.

The usage of composite tshell elements provides a possible remedy for these contradicting demands. To follow this approach, the lay-up of the battery cell is given part-wise with the LS-DYNA® keyword `*PART_COMPOSITE_TSHELL`. Each layer is characterized by material properties and thickness. The structural solver translates the input internally to an integration rule, associating any layer to one of the through the thickness integration points. As a consequence, the lay-up has no effect on the number of degrees of freedom in the system and the thicknesses of the individual layers do not influence the maximum time step for explicit calculations.

As mentioned above, to capture the complex EM and electrochemistry in the battery, a detailed and finely resolved model is required. The EM solver in LS-DYNA uses the composite definition of the

tshell element not as basis of an integration rule but to internally reconstruct a finely resolved model. New degrees of freedom are added to the system, as shown exemplarily in Fig.1. The EM solver invokes an implicit time integration scheme and it can thus be expected that, in contrast to the structural solver and besides the increase in the system of equations, the performance of the solver is only mildly affected by the reconstruction.

The still fairly complex behavior of the individual layers is represented by a so-called “distributed randles circuit” model in LS-DYNA. It has been introduced and discussed in [1, 2] and its extension to the composite thick shell element has been presented in [3]. The element deformation calculated by the structural solver is an input data for this model and one of the result data, namely Joule heating, is computed and handed over to the thermal solver.

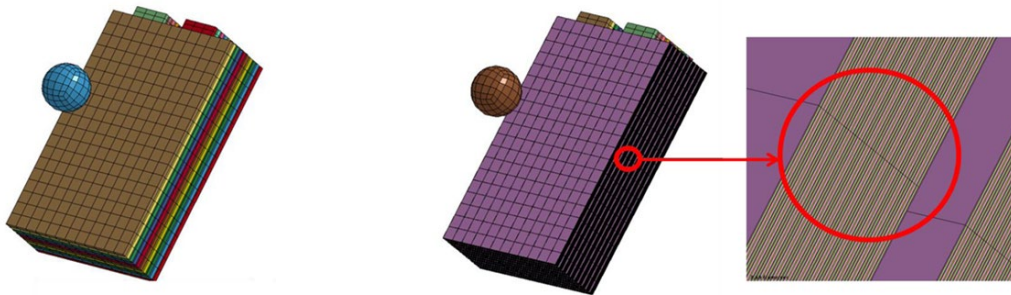


Fig.1: Models of a battery pack from [3]: User mesh with optimal resolution for the structure solver on the left and reconstructed mesh with optimal resolution for EM and thermal solver on the right.

## 2.2 Thermal Element Definition

A similar handling for composite shell elements has been part of the thermal solver in LS-DYNA for some time. A thermal composite tshell element however has been implemented only recently and been presented in [4, 5]. As it is done in the EM solver, the thermal solver internally and automatically reconstructs a fine mesh based on the user defined lay-up within a tshell element.

Naturally, the reconstruction introduces additional virtual elements and virtual nodes and, thus, requires the handling of additional degrees of freedom in the implicit system. The implementation is tested by comparing the temperature evolution in an inhomogeneous stack of solids with the temperature values of an equivalent composite tshell element. In the left of Fig.2 such a validation example with three test cases is depicted. Here, one symmetric solid stack comprises two conductor layers and one insulator layer in between. The thickness of the insulator varies between the different testing scenarios, while the total height of the stack remains constant. The top and bottom segments of the stacks are exposed to different convection boundary conditions. Whereas the environmental temperature at the cold “air” side coincides with the initial stack temperature of 25 °C, the environmental temperatures on the hot “fire” side is assumed to be 800 °C.

Graphs of the temperature evolution on the air side are shown in the right of Fig.2. For a given insulator size the curves obtained with the composite tshell and with a solid stack are in perfect agreement. This indicates that the internal reconstruction of the lay-up works and, thus, that the composite thermal tshell element is able to correctly predict the heat transfer in thickness direction through different layers with different thermal properties.

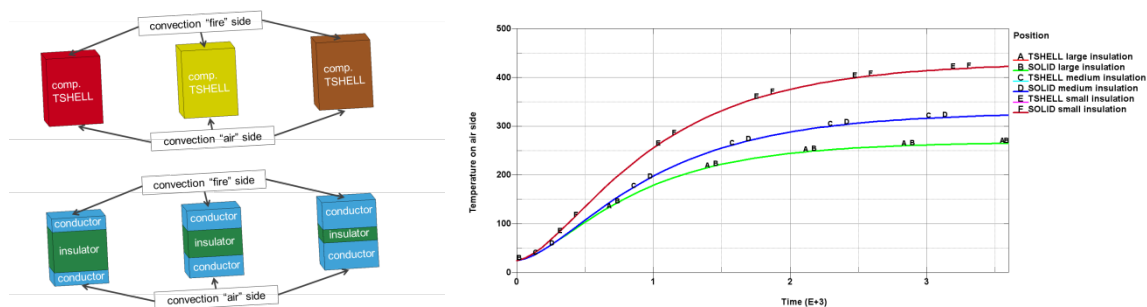


Fig.2: Validation of the thermal composite thick shell against equivalent stacks of solids. Different test cases on the left and resulting temperature evolution for nodes on the “air” side on the right.

As mentioned above the presented development allows for a much easier set-up of the models. But it is important to note that the post-processing of data for the reconstructed meshes is not yet available. So far, temperature data is only output for the nodes of the original mesh (as defined by the user), but no information is available for the virtual nodes yet.

For coupled simulations the information transfer between the solvers has to be ensured. For that purpose, the thermal solver internally links the new virtual nodes generated during the reconstruction to the physical nodes of the initial user mesh and stores that information. This allows providing temperature information for the individual integration points of the tshell elements in the structural solver. The EM solver also keeps similar lists of the mapping between virtual and physical nodes. Although the internal numbering of the virtual nodes and the mapping might differ, it is still possible to share information between EM solver and thermal solver.

To test the implementation of the individual solvers and the interaction of those, various coupled simulation runs have been set-up. Of particular interest is again a comparison between a battery cell modelled with a finely resolved solid mesh and the same cell lay-up represented by composite thick shell element as presented in [6]. That contribution shows that the results of the coupled simulation obtained with a composite definition match the results gained with a fully resolved user mesh.

### 2.3 Contact Capabilities

Many industrial applications and in particular most battery abuse simulations at some point require the simulation tool to deal with complex contact scenarios. In the LS-DYNA structural solver a wide range of well-established contact algorithms is available and can be used for the composite tshell elements. As there are no additional degrees of freedom, the composite lay-up only influences the contact stiffness of the part, but does not require any algorithmic modification.

When considering the heat transfer of a composite part to another part (composite or homogeneous) however, two different contact scenarios have to be distinguished. In the first case the contact zone is at the bottom or top of the thick shell structure, i.e. the nodes of the contact segment all belong to the same layer. For this case the already available and well-established thermal contact routines can be used without further adaptation.

In the second case the heat transfer across the edge of the thick shell structure is of interest, where the lay-up of the structure also has to be considered for at least one contact partner. The heat transfer depends on material, thickness and temperature distribution in the individual layers and, thus, the numerical contact algorithm has to be based on the internal finely resolved model. With the virtual nodes generated by the thermal solver of LS-DYNA the algorithm creates virtual contact segments that are subsequently handed over to the standard contact routines.

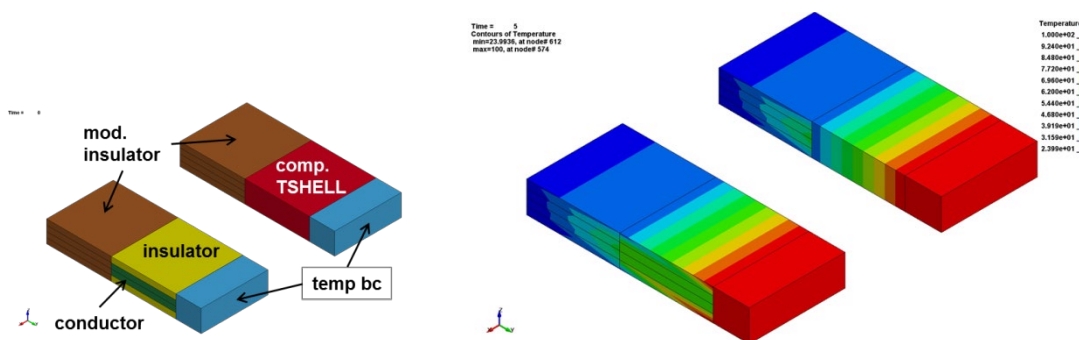


Fig.3: Validation test for contact routines. Mesh and boundary conditions on the left for a composite tshell example and an equivalent solid stack. Resulting temperature distributions on the right.

The capabilities of this approach are demonstrated with the small example shown in Fig.3. Two homogeneous solid blocks are brought in contact with opposite ends of an inhomogeneous structure, with insulator layers on top and bottom and a conductor layer in the middle. The first homogeneous block serves a heat source with prescribed temperatures and the second as “monitor”. For that purpose the material of the latter is characterized by a relatively low thermal capacity and low thermal conductivity and, thus, responds to a spatially varying heat transfer across the contact with an immediate and inhomogeneous temperature change. Two models are compared that differ in the discretization of the inhomogeneous structure in the middle: a stack of four solid elements on the one hand and one composite tshell element with four layers on the other.

The resulting temperature distributions are shown in Fig.3 on the right. First, the result illustrates the limited post-processing capabilities in the current implementation. The lay-up and the resulting inhomogeneous temperature distribution in the stack cannot be visualized in the tshell element. But, second, Fig.3 also demonstrates that temperature distribution in the “monitor” elements is perfect agreement in the two assemblies. Both heat transfer in the contact zones and heat transfer through the composite tshell element work correctly and, in terms of the thermal computation, it does not make a difference if the finely resolved mesh is reconstructed internally or if given by as user input.

### 3 Thermal Boundary Conditions

#### 3.1 Propagation of Boundary Conditions after Element Erosion

In the past few years novel features and specialized boundary conditions have been added for various complex applications of the manufacturing industry c.f. [7, 8, 9]. Nevertheless, most thermal simulations incorporate one or more of the set of “basic” thermal boundary conditions: convection (**\*BOUNDARY\_CONVECTION**), radiation to environment (**\*BOUNDARY\_RADIATION**) or prescribed flux distributed over a surface (**\*BOUNDARY\_FLUX**).

Until recently the only effect of element erosion on these boundary conditions was that segments attached to an eroded element were no longer accounted for. An update of the thermal solver has now enabled these basic thermal boundary conditions to account for newly exposed surfaces after element erosion. To keep the input simple for the user and limit the additional numerical costs, the keywords stated above accept the additional input of a part set. Whenever a solid element that is associated with the part set erodes, any new segment will inherit the boundary condition.

This approach is particularly well suited for applications, in which the element erosion is an effect of the boundary condition itself or at least is initiated at thermally loaded boundary. This is for example the case for laser cutting. It is important to note that the current implementation neither checks for blocking effects nor evaluates if the eroded element belonged to the surface the boundary condition has been originally defined on.

#### 3.2 New Flux Boundary Condition

With the enhancement of the flux boundary condition (**\*BOUNDARY\_FLUX**) described in section 3.1, it would theoretically be possible to simulate laser-cutting applications with LS-DYNA, but the applicability to real processes is strongly limited by the input structure. If at all, important features, such like the motion of the heat source, the shape of the flux region and the effect of tilting of the laser, can only be modelled with user defined functions (**\*DEFINE\_FUNCTION**). For complex geometries and laser paths this is an extremely difficult task.

It is interesting to note that similar considerations have already been made for volumetric heat sources in LS-DYNA to enable their applicability for the simulation of line welding processes. The keyword **\*BOUNDARY\_THERMAL\_WELD\_TRAJECTORY** has been implemented to meet the requirements. It provides an easy input for the motion of a complex volumetric heat source on a complex structure. An overview on the input structure and the capabilities of the feature can be found in [8].

It seemed reasonable to develop a new boundary condition also for heat sources acting on boundary surfaces. The new implementation is addressed as **\*BOUNDARY\_FLUX\_TRAJECTORY**. It uses a similar input structure and incorporates similar features as **\*BOUNDARY\_THERMAL\_WELD\_TRAJECTORY**, of course with the necessary modifications and extensions. For example the new boundary is of course applied on segment sets instead of part sets.

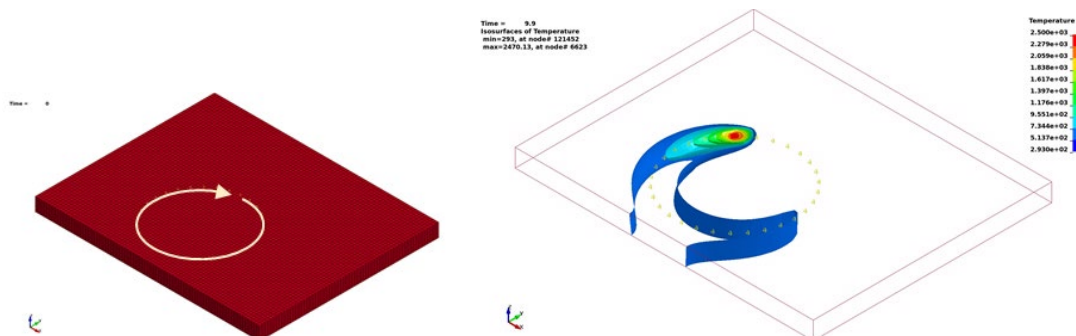


Fig.4: Circular laser motion on a plate: visualization of the path on the left, resulting temperature iso-surfaces on the right together with the node set from the trajectory definition.

The key feature of the new boundary condition is the motion of the heat source along a trajectory with a given velocity. The trajectory is defined by a set of nodes that not necessarily have to be attached to the structure. For example, a circular motion of a laser on a plate is shown in Fig.4. The velocity of the heat source can be defined as function of time. Since trajectory and velocity data are given as input in the keyword, a coupling to the structure solver is not necessary for the definition of the motion. But if the coupling to the structure solver is invoked, the displacements of the nodes of the trajectory and of the boundary segments are of course accounted for.

The trajectory node set defines the center of the heat source. The base shape of the heat source is a double elliptic, the size of which is given in the keyword input. When applied to a surface, the projection of this elliptic defines the zone affected by the heat. Consequently, the current orientation of the heat source has to be defined and tracked during the simulation. Following the concepts of its volumetric counterpart the aiming direction of the heat source in the new boundary condition **\*BOUNDARY\_FLUX\_TRAJECTORY** is a combination of a base orientation and an additional time-dependent rotation around the trajectory.

The crucial quantity for the heating of the boundary is the surface heat density, which is calculated based on the possibly time-dependent total power of the source defined in the keyword and the size of the source (base shape). Additionally, a tilt of the laser with respect to the segment normal reduces the surface heat density, mainly by increasing the surface of the projected area. The keyword aims to reproduce this effect. With an odd value for parameter **ENFO** the boundary condition accounts for the change in area due to the tilt. The effect can be seen for a small example in Fig.5. Furthermore, the user can specify a load curve that defines the reduction of surface heat density as a function of tilt angle. This might be useful to model reflection effects.

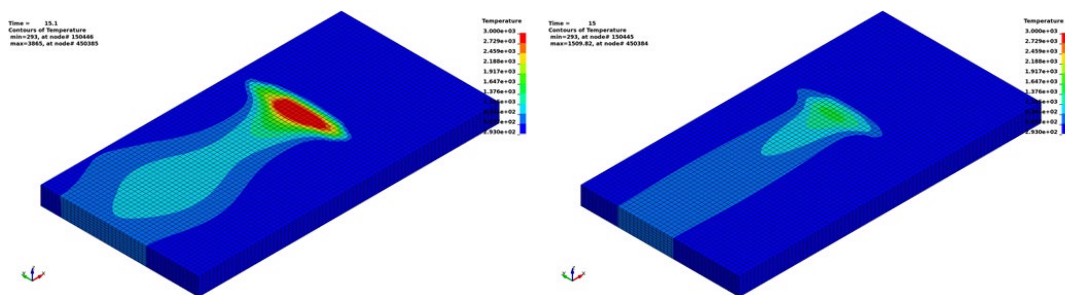


Fig.5: A circular heat source is moving on a block along a straight trajectory. It is cyclically rotated between  $-80^\circ$  and  $80^\circ$  with respect to the surface normal. Pictures show the resulting temperature distributions. On the left, the surface heat density is constant during the process (**ENFO=0**); on the right, it is modified based on the tilt of the source (**ENFO=1**).

The parameter **ENFO** also serves a second purpose. Since the total heat source power is first transferred into a surface density and then integrated numerically over the segments, the resulting total energy rate seen by a structure might not match the user input exactly. Especially for coarse discretizations, there might be a significant deviation. For values of **ENFO** larger than two, the thermal code compensates for this difference by scaling the surface heat density. The scaling factor is calculated internally in every time step and is then used for all segments of the boundary condition.

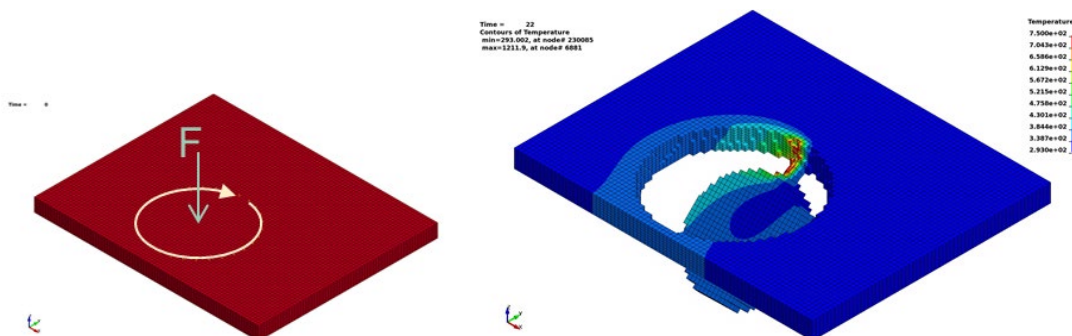


Fig.6: Modified version of example in Fig.4: Element erosion is activated based on a temperature criterion, freshly exposed segments inherit the boundary condition, and a force is applied (left). As a result the laser cuts through eight layers of solid elements (right).

With the approach discussed in section 3.1 the new boundary condition can be propagated to newly exposed surfaces after element erosion. The previous example of the circular trajectory (Fig.4) has been modified: element erosion has been defined based on a maximum temperature criterion and the propagation has been activated. Furthermore, the structure is loaded by a force applied to a node in the inside of the circle. The set-up is depicted in the left of Fig.6 and the results are shown on the right. The laser power in the example is sufficiently large to penetrate eight layers of solid elements and to cut a circular disc from the block.

When the heat input for new boundary segments generated due to element erosion is evaluated, the same projection algorithms as used for the original segments is applied. Thus, the aiming direction of the heat source naturally translates into the cutting direction as is demonstrated with the example presented in Fig.7. A laser with a sufficiently large power moves along a straight trajectory, but it is rotated by 45° with respect to the normal of the affected surface. The evolving cut through the structure reflects this inclination.

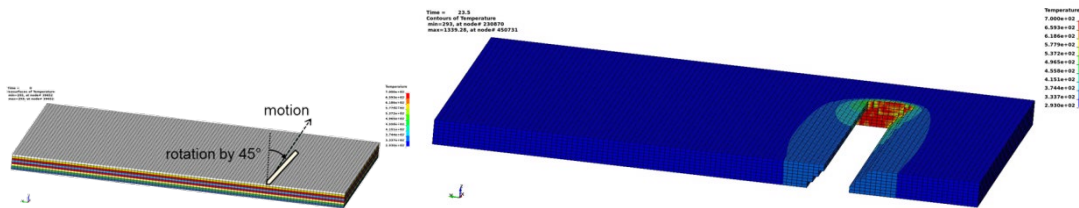


Fig.7: Laser Cutting with a rotated laser beam. Laser travels on a straight trajectory by has a constant rotation angle of 45° with respect to the normal direction surface.

### 3.3 Temperature Boundary Conditions for Resistive Spot Welds

The resistive spot weld (RSW) is the perhaps most commonly used joining process in the automotive industry. Due to the high temperature and locally very high temperature gradients generated during the process, it can cause significant changes in the microstructure found in the heat affected zone (HAZ) and severe deformations in the whole part. The changes in the material properties are of great importance mainly for the crashworthiness of the parts. The distortion naturally influences subsequent steps in the assembly of the structure. For both reasons it seems beneficial to include this welding process into the numerical manufacturing process chain.

From a numerical point of view, the RSW process poses a very complex multi-physics problem that again requires the coupling of the EM, thermal and structure solver in LS-DYNA. The goal is to predict the size of the weld nugget (zone of molten material during the process) and of the HAZ. Feasibility studies with LS-DYNA can be found in [10, 11]. It is not unusual that applications in the automotive industry include hundreds of different spot welds. A detailed coupled numerical analysis of such a large assembly seems impossible and strategies with reduced complexity have to be devised.

One of those simplified approaches has been pursued in the thermal solver of LS-DYNA with the new keyword **\*BOUNDARY\_TEMPERATURE\_RSW**. This boundary condition constrains the temperature degrees of freedom in ellipsoidal region and directly prescribes nodal temperature values. The basic assumption that led to the implementation is that data on weld nuggets, such as size and maximum temperature, are usually available either from a calibration phase or from previous projects. This information can directly be used for the parameterization of the keyword.

The weld nugget is assumed to have the shape of two half ellipsoids, the dimensions of which are defined in the input. The user can also specify a HAZ around the weld nugget. A graphical representation for both options is given in Fig.8.

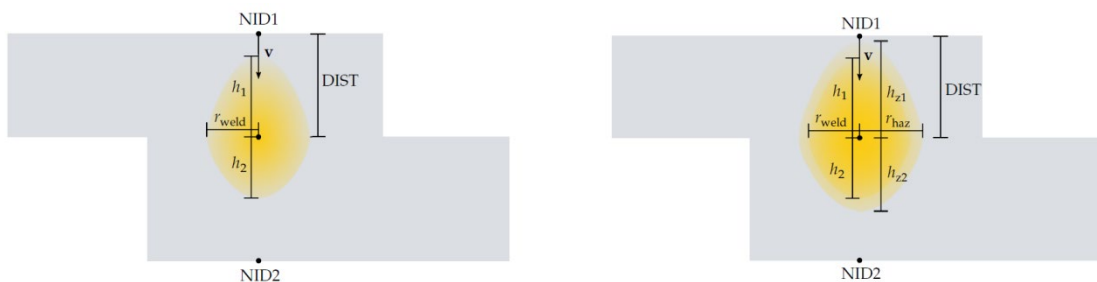


Fig.8: Visualization of the input parameters of **\*BOUNDARY\_TEMPERATURE\_RSW**. On the left, only the weld nugget is specified; on the right also a HAZ is defined

The keyword is applicable to solid and shell elements. A quadratic approximation for the temperature distribution in the weld nugget is assumed requiring the temperature input for the center and at the boundary of the nugget. If the HAZ option is chosen, one additional temperature value for the boundary of this zone is expected. The approximation to the boundary of the nugget is linear.

A small example with only one RSW joining two solid parts is shown in Fig.9. The resulting temperature curve along a horizontal line through the center of the nugget clearly shows the different regions the temperature is prescribed in. Around the center the temperature curve is a quadratic parabola. Outside the nugget the temperature linearly decreases to the boundary of the HAZ. Outside of this zone the temperature is not constraint but a result of the heat transfer equation.

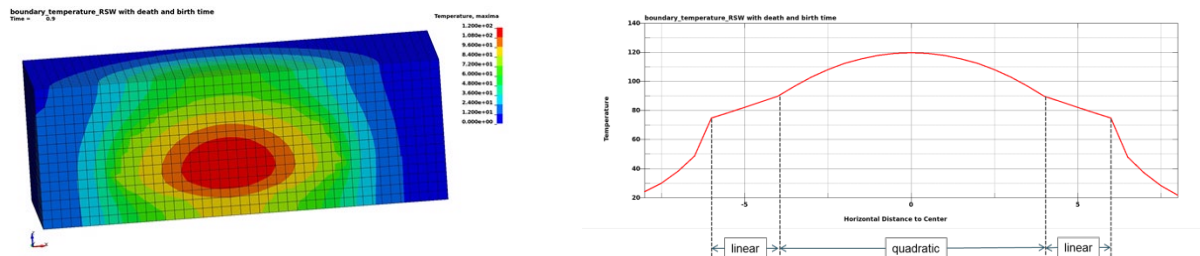


Fig.9: Resulting temperature distribution in a solid block assembled from two parts for a simulation with `*BOUNDARY_TEMPERATURE_RSW` including a HAZ on the left. A graph showing the temperature distribution along a horizontal line through the center on the right.

In the RSW process heat is only generated in a relatively short period of time, when the electrodes are pressed onto the sheets and current is sent through the electrodes. Only for this time range it seems reasonable to prescribe the temperature distribution in the weld region. Before the closing or after the removing of the electrodes, the constraint needs to be removed and the nodal temperatures have to be treated as standard degrees of freedom of the thermal solver. In the keyword input, this is realized by defining birth and death times for activation and deactivation of the boundary condition.

#### 4 Literature

- [1] P. L'Eplattenier, I. Caldichoury, J. Marcicki, A. Bartlett, X. G. Yang, V. Meija, M. Zhu and Y. Chen, „A Distributed Randle Circuit Model for Battery Abuse Simulations Using LS-DYNA,“ in *Proc. of 14th International LS-DYNA Users Conference*, Detroit, 2016.
- [2] S. Bateau-Meyer, P. L'Eplattenier, J. Deng, M. Zhu, C. Bae and T. Miller, „Randles Circuit Parameters Set Up for Battery Simulations in LS-DYNA,“ in *proc. of 15th International LS-DYNA Users Conference*, Detroit, 2018.
- [3] P. L'Eplattenier, „Battery abuse simulations using LS-DYNA,“ in *Proc. of 11th European LS-DYNA Conference*, Salzburg, 2017.
- [4] T. Klöppel und P. Vogel, „Recent Updates to the Structural Conjugate Heat Transfer Solver,“ in *proc. of 15th International LS-DYNA Users Conference*, Detroit, 2018.
- [5] T. Klöppel, „Recent Updates to the Structural Conjugate Heat Transfer Solver,“ in *proc. of 15. German LS-DYNA Forum*, Bamberg, 2018.
- [6] J. Deng, M. Zhu, C. Bae, T. Miller, P. L'Eplattenier und S. Bateau-Meyer, „Safety Modeling of Lithium-ion Batteries under Mechanical Abuse,“ in *proc. of 15th International LS-DYNA Users Conference*, Detroit, 2018.
- [7] T. Klöppel und T. Loose, „Recent developments for thermo-mechanically coupled simulations in LS-DYNA with focus on welding processes,“ in *Proc. of 10th European LS-DYNA Conference*, Wuerzburg, 2015.
- [8] T. Klöppel, „The Structural Conjugate Heat Transfer Solver – Recent Developments,“ in *proc. of 11th European LS-DYNA Conference*, Salzburg, 2017.
- [9] G. Blankenhorn, R. Grimes und F.-H. Rouet, „Current LS-DYNA Developments in Thermal Radiation - `*BOUNDARY_RADIATION_ENCLOSURE`,“ in *proc. in 15th German LS-DYNA Forum*, Bamberg, 2018.

- [10] P. L'Eplattenier, I. Caldichoury, S. Bateau-Meyer, T. Loose und U. Reisgen, „Resistive Spot Welding Simulations Using LS-DYNA,“ in *proc in 11th European LS-DYNA Conference*, Salzburg, 2017.
- [11] I. Caldichoury, P. L'Eplattenier, S. Bateau-Meyer, T. Loose und U. Reisgen, „Update on Resistive Spot Welding Capabilities in LS-DYNA,“ in *proc of 15th International LS-DYNA Users Conference*, Detroit, 2018.